Response to referee 1

A bulk drag parameterizatzion is applied to calculate the aerodynamic roughness length over a part of the western Greenland ice sheet as a function of the surface topography that has been evaluated using UAV photogrammetry and finally ICESat-2 laser altimeter measurements. The parameterization includes skin drag and form drag caused by small scale features such as hummocks and sastrugi. Results for the roughness are compared with those obtained from in situ turbulence measurements. Finally, a map of the surface roughness is presented over a selected region of the western ice sheet. In most parts the paper is very well written and it follows a clear logic presenting novel results. Results might become helpful to better understand in the future the role of surface roughness for atmospheric and ice processes. I suggest, however, an improvement of the description of the used roughness parameterization before publication.

We are grateful to the referee for his thoughtful and precise comments. In the text below we respond point-by-point and discuss the changes to the work. The referee comments are written in black. Our answer to each comment is written below in blue. The proposed changes to the original manuscript are then highlighted in red.

Major Revisions

1. Please separate more clearly in 2.1 the description of the determination of z_{0m} from the measured fluxes and from the used model. Perhaps, introduce corresponding headings so that the structure becomes clear at a first glance.

We agree with the reviewer and therefore propose to add a third sub-section to separate the definition of z_{0m} from the bulk model for z_{0m}.

L60:

2 Model

2.1 Definition of the aerodynamic roughness length z_{0m}

(...)

Hence, the process of finding z_{0m} is equivalent to finding d, $\frac{u(z)}{u_*}$ and $\widehat{\Psi_m(z)}$ simultaneously.

2.2 Bulk drag model of z_{0m}

The main task is to model the total surface shear stress $\tau = \rho u_*^2$, which for a rough surface is the sum of both form drag τ_r and skin friction τ_s:

(...)

2.3 Definition of the height (H) and frontal area index (λ) over a rough ice surface
(...)

2. It seems that a mixture is used here of the schemes by R92, Andreas (1995) and of own assumptions. E.g., equation (A3) ignores the wake effect. Please compare this with equation (7) of Andreas (1995). This needs explanation. Please clearly specify own assumptions.
The reviewer is right, we have applied the R92 model to a realistic surface (rough ice), just as Andreas (1995) did for sastrugi. Our equation (A3) is in fact Equation (12) from R92, which aims to model the skin friction for a flat surface without any obstruction by roughness elements. However in this study we do take into account wake effects that occur when $\lambda > 0$ as in Andreas (1995), in our equation (A7). We have added clarification with our Equations (A3) and (A7) and hope this becomes more clear in the revised manuscript.

L428:
Similarly, R92 models the skin friction for an unobstructed flat surface as:

$$\lim_{\lambda \to 0} \tau_s = \rho C_s(z) u(z)^2 \tag{A3}$$

L445:
Based on the previous work of Arya (1975), and on scaling arguments of the effective shelter volume, R92 includes sheltering and models the total surface shear stress over multiple obstacles as:

$$\begin{aligned} \tau(\lambda) &= \tau_s(\lambda) + \tau_r(\lambda) \\ &= \rho u(H)^2 \left[C_s(H) \exp\left(-c\lambda \frac{u(H)}{u_*} \right) + \lambda C_d \exp\left(-c\lambda \frac{u(H)}{u_*} \right) \right], \end{aligned} \tag{A7}$$

where $c = 0.25$ is an empirical constant that determines the sheltering efficiency.

3. In its present version equation (A4) is wrong. This can be seen by inserting the value z = 10 m. Probably, a missprint (?)

The reviewer is correct, there are two misprints in our equation (A4). The height of the obstacles H should be replaced by the variable z. A minus sign was also missing in the exponent of $C_s(10)$. The correct version of the equation was used in the code, therefore this does not affect the results in any way. We have corrected these misprints in the revised version.
L429
Following Andreas (1995), $C_s(z)$ is estimated from the 10-m drag coefficient

$C_s(10)$ measured over a flat surface, according to:

$$C_s(z) = \left[C_s(10)^{-0.5} - \frac{1}{\kappa} \left(\ln \left(\frac{10-d}{z-d} \right) - \widehat{\Psi_m}(z) \right) \right]^{-2}, \qquad \text{(A4)}$$

with $C_s(10) = 1.2071 \times 10^{-3}$, which yields $z_{0m} = 10^{-4}$ m for a perfectly flat surface in this model.

4. I understood that $\widehat{\Psi_m(z)}$ is set to zero to derive z_{0m} from measurements. But this differs from the assumptions in the Appendix for the most complex scheme. Please better explain why this is no contradiction.
Using the bulk drag model of R92, the estimation of z_{0m} requires modelling the drag coefficient, thus the wind speed and the momentum flux, at the top of the roughness elements ($z = H$). At this height the averaged vertical profiles of horizontal wind velocity deviate from the inertial sublayer wind profile by an offset $\widehat{\Psi_m(z)}$. However for $z > 2H$ we assume that the inertial sublayer profile is valid again, and defined by a roughness length z_{0m}. Thus, linking the z_{0m} that defines the wind profile in the inertial sublayer ($z > 2H$) to the wind speed at the top of the roughness elements ($z = H$) requires correcting for the wind profile deviation by $\widehat{\Psi_m(z)}$. On the other hand, when estimating z_{0m} from the measured wind speed and momentum flux, we assume that the instruments are located in the inertial sublayer where $\widehat{\Psi_m(z)} = 0$. This is most likely valid, given that we measure at $z = 3.7$ m and that $H < 1.5$ m at measurement site S5. We propose to add an explanatory sentence in our section *3.1 Eddy covariance measurements*:

L156
We only select data taken during near-neutral conditions ($z/L_o < 0.1$), and we assume that the measurements are taken above the roughness layer, i.e. $\widehat{\Psi_m(z)} = 0$. The latter is a reasonable assumption, given that the height of the obstacles (H) at these sites is less than 1.5 m, which means that the roughness layer unlikely exceeds 3 m (Smeets et al., 1999; Harman and Finnigan, 2007). On the other hand, when applying the drag model to estimate z_{0m} (Appendix A.), the correction factor $\widehat{\Psi_m(z)}$ is taken into account. The reason is that the obstacles are located in the roughness layer, where the vertical wind profiles deviate from the inertial sublayer wind profiles, according to Eq. (1).

5. I propose to describe in the Appendix first the complete scheme by R92 (in its version used here), and then give equations (A5) and (A6) of others. This would facilitate reading.
We agree with the reviewer, and we have moved equations (A5) and (A6) to the end of Appendix A.

L467:

Other attempts have been made to relate z_{0m} to the geometry of multiple surface roughness elements. For instance Lettau (1969, L69) empirically relates z_{0m} to the average frontal area index of the roughness obstacles, which has been adapted by Munro (1989) for the surface of a glacier:

$$z_{0m,L69} = 2C_d H \frac{A_f}{A_l} = 2C_d H \lambda. \tag{A13}$$

Macdonald et al. (1998,M98) have shown that Eq. (A13) can be obtained by assuming that there is only form drag, and by setting $d = 0$, $\widehat{\Psi_m(z)} = 0$ and $C_d = 0.25$. By including the displacement height d, M98 is able to reproduce the non-linear feature of the $\frac{z_{0m}}{H} = f(\lambda)$ curve:

$$z_{0m,M98} = (H-d)\exp\left(-\left[\frac{C_d}{\kappa^2}\lambda\left(1-\frac{d}{H}\right)\right]^{-0.5}\right). \tag{A14}$$

[*end of Appendix A*]

6. The obstacle height is set twice the standard deviation of the filtered profile. How sensitive are the results to this assumption?

The elevation profiles we consider contain information at all wavelengths. Therefore, changing the value of the high-pass cutoff wavelength affects the resulting standard deviation, and thus the modelled value for z_{0m}. We propose to add a sensitivity analysis on the modelled H, λ and z_{0m} for $\Lambda \in [10; 50]$ m at site S5 in the new Appendix B (see Fig B1). We also propose to add a few explanatory sentences in the Appendix regarding this sensitivity.

L113:
To remove the influence of the widest obstacles, the elevation profile of length L is linearly detrended and the power spectral density of the detrended profile is computed in order to filter out all the wavelengths larger than the cutoff wavelength $\Lambda = 35$ m. This value is found to give optimal results, which is shown in Appendix B.

Appendix B: Sensitivity experiments:

Cutoff wavelength Λ

We find that the optimal value of the cutoff wavelength for the high-pass filter is $\Lambda = 35$ m. This may be explained by the fact that the resulting filtered topography using $\Lambda = 35$m still contains most (≈ 80 %) of the total variance of the slope spectrum. The latter is defined as the power spectral density of the first derivative of the elevation profile. A sensitivity experiment using different values for Λ at S5 can be found in Fig. B1. Changing the value for Λ strongly impacts the estimated H (Fig. B1c), as the elevation profiles considered here contain information at all wavelengths (Fig. B1a). On the other hand, increasing the value for Λ above 35m does not significantly affect the estimate frontal

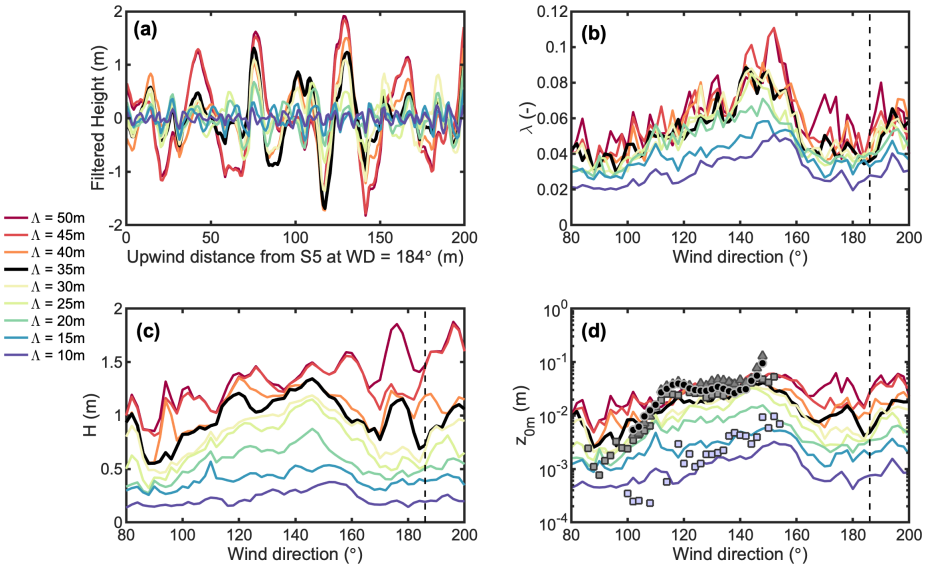

Figure B1: (a) Filtered elevation profile in wind fetch direction 186°, (b) estimated obstacle frontal aera index, (c) estimated obstacle height and (d) modelled aerodynamic roughness length at site S5 for different high-pass cutoff wavelengths Λ. See Figure 8 in main text for the labels in d).

area index λ (Fig. B1b). Overall, increasing Λ from 10 m to 50 m increases the modelled z_{0m} from 7.6×10^{-4} m to 2.8×10^{-2} m at S5, in the wind fetch direction 184° that matches the ICESat-2 track (Fig. B1d).

7. Equation (A2) (upper line) has been given in Garbrecht et al. (2002) (not Garbrecht et al. (1999) as in the lower line).
The reviewer is right. We have modified the reference accordingly.

L423:
Based on the analysis by Garbrecht et al. (2002) for sea-ice pressure ridges, we choose the following parameterization,

$$C_d = \begin{cases} \frac{1}{2}(0.185 + 0.147H) & \text{if } H \leq 2.5 \text{ m} \\ \frac{1}{2}\left(0.22\log(\frac{H}{0.2})\right) & \text{if } H > 2.5 \text{ m} \end{cases} \quad \text{(A2)}$$

Note that the factor 1/2 is a consequence of a different definition for C_d in Garbrecht et al. (2002) than Eq. (A1).

8. Line 80: Equation (3) is used by Lüpkes et al. (2012) and by Lüpkes and Gryanik (2015) as well. The difference is that the width of the roughness elements (ice floes) can be of the same order as the width of open water fetch. However, exactly the same equation (3) is used by Garbrecht et al. (1999, 2002) and by Castellani et al. (2014), who parameterize the impact of ridges on sea ice. The difference in their models to the one discussed in the manuscript is that due to the large distances between ridges further simplifications are possible.
We thank the reviewer for this clarification. We believe this information might be useful for the interested reader, and thus we propose the following modification :

L84:
At this point, we will differ from the model by Shao and Yang (2008), who add an extra term in Eq. (3) in order to separate the skin friction at the roughness elements and the underlying surface. We also differ from the models by Lüpkes et al. (2012) and Lüpkes and Gryanik (2015), where skin friction over sea-ice is separated between a component over open water, and a component over ice floes. In the case of a rough ice surface, their is no clear distinction between the obstacles and the underlying surface. Therefore, we follow the model of Raupach (1992, R92), which is designed for surfaces with a moderate frontal area index ($\lambda < 0.2$).

9. Figure 6: It should be mentioned that the 'observed' z_{0m} depends also on a model, namely on all assumptions involved in equation (2) when it is applied over inhomogeneous surface topography. This would be different if just drag coefficients were compared with each other, for which just the observed wind speed and momentum fluxes at the measurement height would be needed.
We agree with the reviewer. We propose to replace the "measured z_{0m}" by "estimated z_{0m} from in situ observations" everywhere in the text and in figure

captions.

Minor Revisions

1. Line 32: here it might be useful to cite cite also Lüpkes and Gryanik (2015).
Added

L32
Lüpkes et al. (2012) and Lüpkes & Gryanik (2015) developed a bulk drag model for sea-ice that is used in multiple atmospheric models.

2. Line 36: perhaps after 'the application of such models' in weather and climate models.
Changed

L36
The second challenge is the application of such models in weather and climate models, which requires mapping small-scale obstacles over large areas, e.g. an entire glacier or ice sheet.

3. Section 2.1, the hat over Ψ_m should always appear as in equatuion (1).
We have chosen to use the notation from Harman and Finnigan (2007), where the hat notation is used for roughness sublayer variables. Therefore Ψ_m and $\widehat{\Psi_m(z)}$ are two distinct quantities. We propose an extra sentence in Section 2.1 for clarification.

L71
The dependency of the eddy diffusivity for momentum on the diabatic stability and on the turbulent wake diffusion are described as $\Psi_m\left(\frac{z-d}{L_o}\right)$ and $\widehat{\Psi_m(z)}$, respectively, where L_o is the Obukhov length. The hat notation is used for the roughness layer quantities, as in Harman and Finnigan (2007).

4. Figure 6, caption: The solid grey symbols are not really measurements of z0. These points have probably been derived from wind and flux measurements applying equation (2). That's a large difference because equation (2) is also a kind of model. Please, add also equation numbers for the different z_{0m} data.
In accordance with previous Major comment #9, we propose to replace all the "measured z_{0m}" by "estimated z_{0m} from in situ observations".

5. Line 273: one could add here that also Lüpkes et al. (2012) use constant Cd (which is cw in their paper).
added

L274
The parametrization for Cd from Garbrecht et al. (1999) (Eq. (A2)), for which Cd increases with H, yields most acceptable results when used in combination with the R92 model (Fig. 6). Note that Lüpkes et al. (2012) use a constant value for C_d.

6. line 315: compare H and λ .... you mean: compare with satellite and UAV measurements?
Yes. We have modified the sentence for clarification.

L315
Although the UAV profile is too short to statistically compare H and λ to the ICESat-2 altimeter, the qualitative comparison between the two confirms that the satellite altimeter is very well capable of detecting most of the obstacles that are smaller than 20 m in width.

7. Figure 8: I do not understand the shift of the orange dotted line. Perhaps I have overseen the explanation? Also in the caption, which modelled z_{0m}? There are several approaches....
The orange dotted line is the orange line divided by 10, and is therefore a crude guess of what the modelled z_{0m} using UAV data would look like at site S5 in March. We propose to add an explanatory sentence. We also detailed which model was used in the caption. Note that we have also separated Fig. 8 in two parts, after a suggestion by Referee #3.

L319
Both H and λ are smaller in the satellite profile than in the UAV profile, but the modelled z_{0m} agrees qualitatively with the z_{0m} estimated from AWS S5 measurements during March-April. During this time period, z_{0m} is approximately a factor 10 smaller than during the end of the ablation season (Fig. 8, dashed orange line).

8. line 334: 'between different in situ' ? Forgotten data?
Corrected

L334:
The difference between different in situ data highlights the variability in z_{0m} in time, but also the uncertainty in the field measurements.

9. line 337: better write somethink like: hummocks having been formed during westerly wind have usually ....
We do not discuss how the ice hummocks have been formed, which is outside the scope of this paper. Nevertheless the surface at S5 may be considered as homogeneously covered by nearly identical yet anisotropic ice hummocks, that have different heights and frontal area indices depending on the looking direction. We

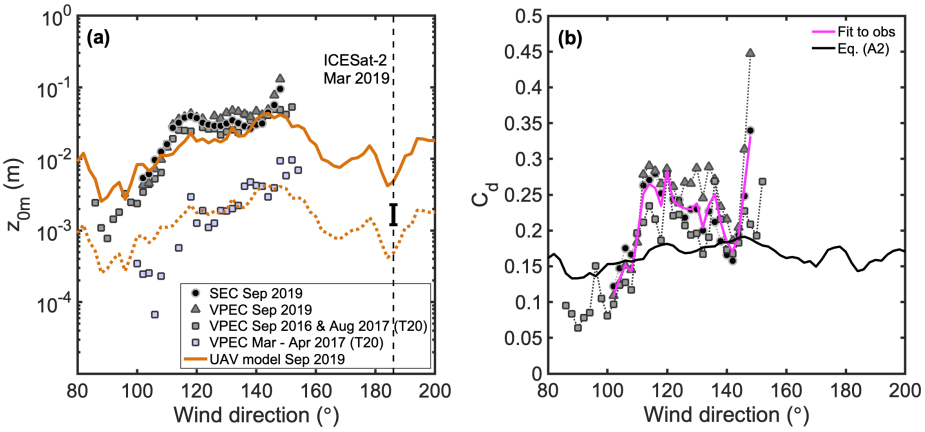

Figure 8: (a) Drag model evaluation at site S5. (b): Drag coefficient for form drag (C_d) used in the bulk drag model (black line) or required to perfectly fit the observations. The orange solid line is the modelled z_{0m} using the R92 model and UAV photogrammetry on 06 September 2019, while the dashed orange line is the orange line shifted down by a factor 10. Solid symbols are measurements from sonic eddy-covariance (SEC) or vertical propeller eddy-covariance (VPEC). Additional data is from van Tiggelen et al. (2020, T20). The vertical dashed line denotes the direction sampled by the ICESat-2 laser beam on 14 March 2019. The errorbar denotes the range between the uncorrected and corrected ICESat-2 measurements.

propose some minor changes in the revised manuscript for clarification. We also propose to update "westerly wind direction" in "easterly wind fetch direction".

L337:
The ice hummocks seen in the easterly wind fetch directions have smaller H and λ, which results in a smaller z_{0m} than the hummocks seen in the southerly wind fetch directions. This is due to the anisotropic nature of the ice hummocks.